Lithogeochemical re-analysis of British Columbia Geological Survey archived rock samples from northwestern British Columbia

Jackie Van der Vlugt
Alexei S. Rukhlov
Bram I. van Straaten

BRITISH COLUMBIA
Ministry of
Energy, Mines and
Low Carbon Innovation

Confidential until January 23, 2023

GeoFile 2022-14

Ministry of Energy, Mines and Low Carbon Innovation
Mines, Competitiveness, and Authorizations Division
British Columbia Geological Survey

Recommendation citation: Van der Vlugt, J., Rukhlov, A.S., and van Straaten, B.I., 2022. Lithogeochemical re-analysis of British Columbia Geological Survey archived rock samples from northwestern British Columbia. British Columbia Ministry of Energy, Mines and Low Carbon Innovation, British Columbia Geological Survey GeoFile 2022-14, 15p.

Ministry of
Energy, Mines and
Low Carbon Innovation

Lithogeochemical re-analysis of British Columbia Geological Survey archived rock samples from northwestern British Columbia

Jackie Van der Vlugt
Alexei S. Rukhlov
Bram I. van Straaten

Ministry of Energy, Mines and Low Carbon Innovation
British Columbia Geological Survey
GeoFile 2022-14

Lithogeochemical re-analysis of British Columbia Geological Survey archived rock samples from northwestern British Columbia

Jackie Van der Vlugt[1a], Alexei S. Rukhlov[1a], Bram I. van Straaten[1]

[1] British Columbia Geological Survey, Ministry of Energy, Mines and Low Carbon Innovation, Victoria, BC, V8W 9N3
[a] corresponding authors: jackie.vandervlugt@gov.bc.ca, alexei.rukhlov@gov.bc.ca

Recommendation citation: Van der Vlugt, J., Rukhlov, A.S., and van Straaten, B.I., 2022. Lithogeochemical re-analysis of British Columbia Geological Survey archived rock samples from northwestern British Columbia. British Columbia Ministry of Energy, Mines and Low Carbon Innovation, British Columbia Geological Survey GeoFile 2022-14, 15p

Abstract

Whole-rock re-analysis of archived samples mainly from Stikine terrane in northwestern British Columbia can help better understand the magmatic and geochemical evolution of the region and evaluate its prospectivity. From the British Columbia Geological Survey (BCGS) archive, we retrieved a suite of 946 samples for re-analysis. These samples, predominantly Triassic to Jurassic igneous rocks but including a range from Devonian to Quaternary, were collected between 1985 and 2021 mostly for petrogenetic studies (775) or for determination of metal contents in altered and mineralized rocks (171). The re-analysis included determinations for 60 analytes using four-acid digestion with a combination of inductively coupled plasma atomic emission spectroscopy (ICP-AES) and inductively coupled plasma mass spectrometry (ICP-MS) for ultra-low minimum detection limits. In addition, 498 samples that lacked modern determinations were re-analyzed for 56 analytes using lithium-borate fusion with ICP-AES or ICP-MS finish with ultra-low minimum detection limits, and for LOI at 1000 °C gravimetrically. Quality of the new data is evaluated based on 87 blind quality controls. A comprehensive geoscientific metadata structure captures full bedrock geological unit and sample information from the original source.

Keywords: Whole-rock lithogeochemistry, northwestern British Columbia, Stikine terrane, igneous rocks, petrogenesis, alteration, mineralization, quality control, four-acid digestion, lithium-borate fusion, ICP-AES, ICP-MS, ultra-low minimum detection limits, Betty Creek Formation, Bowser Lake Group, Cone Mountain Plutonic Suite, Edontenajon formation, Forrest Kerr Plutonic Suite, Galore plutonic suite, Gnat Lakes plutonic suite, Hazelton Group, Hluey Lakes complex, Horn Mountain Formation, Hyder Plutonic Suite, Iskut River Formation, Kinskuch unit, Kitsault unit, Klastline formation, More Creek Plutonic Suite, Nickel Mountain plutonic suite, Quock Formation, Sloko Group, Snowdrift Creek plutonic suite, Spatsizi Formation, Stikine assemblage, Stikine Plutonic Suite, Stuhini Group, Sustut Group, Tatogga plutonic suite, Texas Creek Plutonic Suite, Three Sisters Plutonic Suite, Tsaybahe group

1. Introduction

In the last 30 years, the British Columbia Geological Survey (BCGS) has conducted geologic mapping and mineral deposit studies in the northwestern part of the province, generating a significant archive of rock samples. From the BCGS archive we selected 946 rock samples for re-analysis using 4-acid digestion and lithium-borate fusion (Fig. 1) by ALS Canada Ltd. In the full dataset (BCGS_GF2022-14.zip), Appendix 1 contains all sample metadata and lithogeochemical data (**1a**, new data; **1b**, published data; **1c**, combined new and selected published data; **1d**, explanation of headers; **1e**, references) and Appendix 2 contains all original analytical certificates, including quality control data from ALS.

2. Sample distribution and geology

Predominantly plutonic and volcanic rock samples chosen for re-analysis range from Devonian to Quaternary and are mainly from the Stikine terrane (Fig. 2). Most samples were collected in the Dease Lake, Kitsault River, Galore Creek, Telegraph Creek, Forrest Kerr-Mess Creeks, and upper Iskut River areas. For further geologic information see: 1) Dease Lake (Logan et al., 2012; van Straaten et al., 2012, 2022b); 2) Kitsault River (Hunter and van Straaten, 2020; Miller et al., 2020; Hunter et al., 2022); 3) Galore Creek (Logan and Koyanagi, 1994; Logan, 2005); 4) Telegraph Creek (Brown et al., 1996); 5) Forrest Kerr-Mess Creek area (Logan et al., 2000; Logan, 2004); and 6) upper Iskut River (Ash et al., 1997;

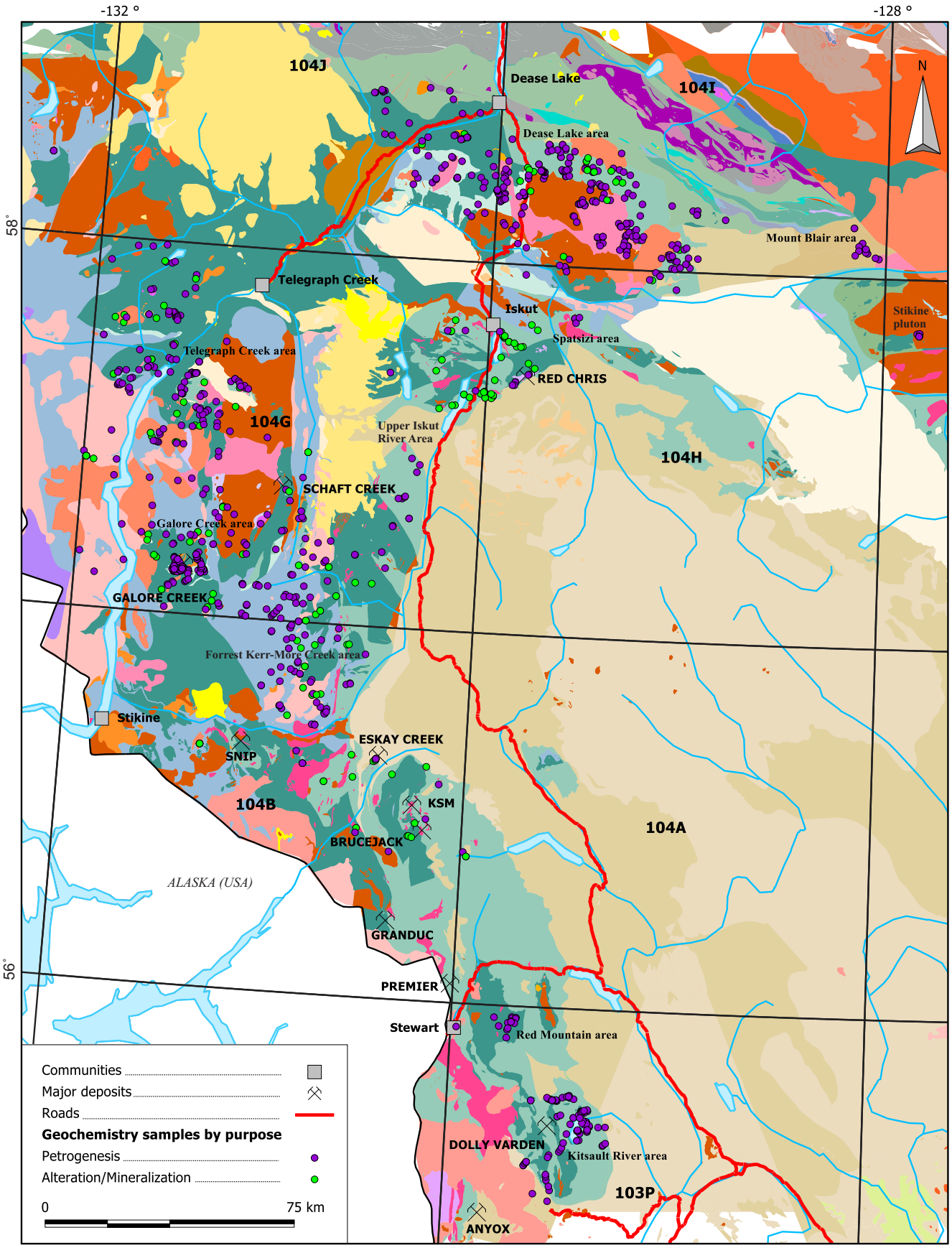

Fig. 1: Sample location map; geology from BC Digital Geology version 2021-10-06 (Cui et al., 2017).

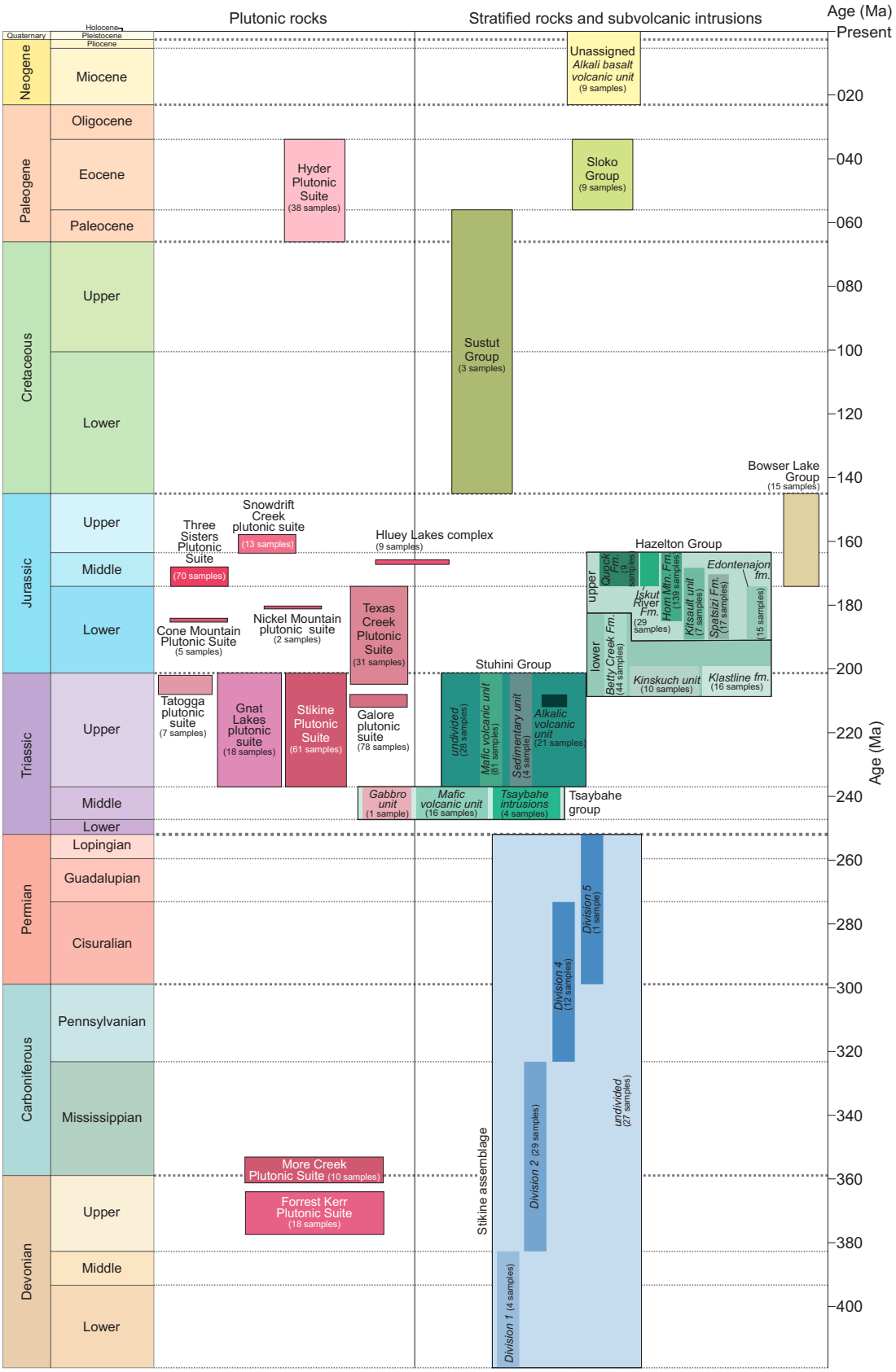

Fig. 2: Schematic Devonian to Quaternary stratigraphic and magmatic framework displaying unit assignments for 908 out of 946 routine lithogeochemistry samples. Names at the rank of group or suite in large font, names at the rank of formation or lithodeme in smaller italic font. Geological timescale after Cohen et al. (2013).

Alldrick et al., 2006; Nelson et al., 2018).

3. Archived sample retrieval, preparation, and analytical methods

3.1 Samples

A total of 946 archived samples from northwestern British Columbia were selected for re-analysis. The samples were selected based on location, rock type, and sample description, with priority given to least-altered igneous rocks, followed by altered and/or mineralized igneous samples. Sample locations and descriptions were obtained from the provincial rock geochemical database (Han et al., 2016; Han and Rukhlov, 2020) and original data sources (e.g., van Straaten et al., 2022a), and checked for consistency with the BC digital geology database (Cui et al., 2017). Petrogenesis samples (779) include most samples (552) in van Straaten et al. (2022a), except a few possible duplicates and samples missing in the archive. We also searched the provincial rock geochemical database (Han et al., 2016; Han and Rukhlov, 2020) for samples with major-element concentrations determined by X-ray fluorescence (XRF) or fusion with ICP-AES, which yielded an additional 227 samples. The laboratory numbers of these additional samples were retrieved from the BCGS laboratory records, and we checked for sample availability of material in the BCGS sample archive. For alteration and/or mineralization samples (167), which typically lacked major-element determinations, only those mapped as being in igneous map units and described as having igneous protoliths were considered further.

3.2. Geoscientific metadata

This release provides detailed geoscientific metadata for all samples; the metadata allow for full capture and querying of bedrock geological unit information such as geological age, numerical age or age range, group or suite name, formation or lithodeme name, and member or phase name (see van Straaten et al., 2022a for details). Metadata for 552 out of 946 routine samples are from van Straaten et al. (2022a). For the remainder of the samples, metadata were populated based on information in the provincial rock geochemical database (Han et al., 2016; Han and Rukhlov, 2020), original source publications and/or BC digital geology. The reliability of unit assignments (*strat_unit_reliability* field, see Appendix 1) is typically considerable or high for petrogenesis samples. For samples collected for characterization of alteration or mineralization, the reliability of unit assignments is typically low to moderate, because original field descriptions commonly focus on describing alteration and/or mineralization and have limited information on the protolith. In addition to the fields included in van Straaten et al. (2022a), we also populated a *rock_name* field based on the sample descriptions.

To ensure consistency throughout the entire data set and alignment with updated stratigraphic nomenclature, we renamed Polaris ultramafic suite to Gnat Lakes plutonic suite, Copper Mountain Plutonic Suite to Galore plutonic suite, Sloko-Hyder Plutonic Suite to Hyder Plutonic Suite, McClymont Plutonic Suite to Forrest Kerr Plutonic Suite and Nickel Mountain suite to Nickel Mountain plutonic suite. In cases where no group or suite name (*gp_suite* field, Appendix 1) was available, we used 'Unassigned' to avoid blank fields. We introduced several informal, temporary, and descriptive unit names in the formation/lithodeme (*fm_lithodm*) and member/phase (*mem_phase*) fields to increase the user's ability to filter by *strat_name* (e.g., Stuhini Group – Mafic volcanic unit). We subdivided the Stikine assemblage into informal Divisions 1, 2, 4, and 5 as proposed by Logan et al. (2000). Galore intrusions were subdivided into twelve informal phases (I-1 to I-12) following Enns et al. (1995). Samples from subvolcanic intrusions were typically assigned to the stratigraphic group and/or formation that the intrusions are interpreted to have fed (following North American Commission on Stratigraphic Nomenclature, 2005), but with a distinct name at a lower rank (using either the *fm_lithodm* or *mem_phase* fields; e.g., Tsaybahe group – Tsaybahe intrusions). Where only a few subvolcanic intrusions were sampled, they are included with the volcanic unit that they are interpreted to have fed.

The re-analysis program includes data from a commonly remote and mountainous area extending for about 54,600 km^2. In many cases bedrock unit assignments are based on low- to moderate-density field observations, and ages are underpinned by limited paleontological and geochronological data. Petrographic studies have only been reported for a subset of samples (e.g., Brown et al., 1996; van Straaten et al., 2022a). Furthermore, unit assignments have not been evaluated using the lithogeochemical data presented herein. As such, most unit assignments should be treated as preliminary. Mineral abbreviations used throughout Appendix 1 are after Siivola and Schmid (2007).

3.3 Sample preparation

The samples were retrieved from the BCGS sample archive and checked for integrity. Only uncompromised materials, sufficient for re-analysis, were split and prepared at the BCGS laboratory in Victoria. Of the 946 routine samples, 633 were already pulverized and did not require further preparation, whereas 313 required pulverizing. Most of the archived rock pulps were originally prepared with a tungsten carbide ring and puck mill at BCGS, some were pulverized using chromium steel mill (BCGS), and others using a mild steel mill at a different laboratory.

For the samples requiring preparation, a tungsten carbide ring and puck mill was used for the initial 15 samples; a chromium steel ring and puck mill was used for the remaining 298 samples. The samples were pulverized for 20 seconds, followed by screening to ensure 100% passing through 200 mesh (75 µm) on a stainless steel sieve. To minimize cross contamination, we used a silica wash between samples. The pulps were split into 10 g and 2 g aliquots for analysis by methods detailed below. In addition, 127 of the 633 archived pulps were sieved to recover material 100% passing through a 200-mesh screen before splitting.

3.4 Analytical methods

All samples in this release were analyzed by ALS Canada Ltd; Tables 1 and 2 list the analytes and detection limits for each method. The analysis involved four-acid (4A) digestion, with samples that lacked modern (post-2010) total determinations (498 samples) also analyzed using a lithium-borate fusion technique. The 4A technique digests a 0.25 g sample in a mixture of concentrated $HNO_3 + HClO_4 + HF$ acids (1.5 mL) at 185 °C, followed by evaporation of the solution

Table 1. Analytes and detection limits by four-acid digestion with an ICP-AES or ICP-MS finish (ALS Canada Ltd. method code ME-MS61L and MS61L-REE add-on).

Analyte	Units	Lower limit	Upper limit	Analyte	Units	Lower limit	Upper limit	Analyte	Units	Lower limit	Upper limit
Ag	ppm	0.002	100	**Hf**	ppm	0.004	500	**Sb**	ppm	0.02	10000
Al	wt%	0.01	50	**Ho**	ppm	0.002	1000	**Sc**	ppm	0.01	10000
As	ppm	0.02	10000	**In**	ppm	0.005	500	**Se**	ppm	0.006	1000
Ba	ppm	1	10000	**K**	wt%	0.01	10	**Sm**	ppm	0.004	1000
Be	ppm	0.02	1000	**La**	ppm	0.005	10000	**Sn**	ppm	0.02	500
Bi	ppm	0.002	10000	**Li**	ppm	0.2	10000	**Sr**	ppm	0.02	10000
Ca	wt%	0.01	50	**Lu**	ppm	0.002	1000	**Ta**	ppm	0.01	500
Cd	ppm	0.005	1000	**Mg**	wt%	0.01	50	**Tb**	ppm	0.002	1000
Ce	ppm	0.01	500	**Mn**	ppm	0.2	100000	**Te**	ppm	0.005	500
Co	ppm	0.005	10000	**Mo**	ppm	0.02	10000	**Th**	ppm	0.004	10000
Cr	ppm	0.3	10000	**Na**	wt%	0.001	10	**Ti**	wt%	0.001	10
Cs	ppm	0.01	500	**Nb**	ppm	0.005	500	**Tl**	ppm	0.002	10000
Cu	ppm	0.02	10000	**Nd**	ppm	0.005	1000	**Tm**	ppm	0.002	1000
Dy	ppm	0.005	1000	**Ni**	ppm	0.08	10000	**U**	ppm	0.01	10000
Er	ppm	0.004	1000	**P**	wt%	0.001	1	**V**	ppm	0.1	10000
Eu	ppm	0.004	1000	**Pb**	ppm	0.01	10000	**W**	ppm	0.008	10000
Fe	wt%	0.002	50	**Pr**	ppm	0.004	1000	**Y**	ppm	0.01	500
Ga	ppm	0.05	10000	**Rb**	ppm	0.02	10000	**Yb**	ppm	0.004	1000
Gd	ppm	0.005	1000	**Re**	ppm	0.0004	50	**Zn**	ppm	0.2	10000
Ge	ppm	0.05	500	**S**	wt%	0.01	10	**Zr**	ppm	0.1	500

Note: over-limit results for Ag, Cu, Pb, and Zn were determined using four-acid digestion with ICP-AES finish.

Table 2. Analytes and detection limits by lithium-borate fusion digestion with an ICP-AES or ICP-MS finish (ALS Canada Ltd. method codes ME-ICP06 and ME-MS81s) and gravimetric loss on ignition (LOI) at 1000 °C for one hour (ALS Canada Ltd. method code OA-GRA05).

Analyte	Units	Lower limit	Upper limit	Analyte	Units	Lower limit	Upper limit	Analyte	Units	Lower limit	Upper limit
SiO_2	wt%	0.01	100	**Cr**	ppm	3	10000	**Pr**	ppm	0.02	1000
TiO_2	wt%	0.01	100	**Cs**	ppm	0.04	10000	**Rb**	ppm	0.1	10000
Al_2O_3	wt%	0.01	100	**Cu**	ppm	3	10000	**Sc**	ppm	0.2	500
Cr_2O_3	wt%	0.002	100	**Dy**	ppm	0.02	1000	**Sm**	ppm	0.01	1000
Fe_2O_3(T)	wt%	0.01	100	**Er**	ppm	0.02	1000	**Sn**	ppm	0.5	10000
MnO	wt%	0.01	100	**Eu**	ppm	0.01	1000	**Sr**	ppm	0.2	10000
MgO	wt%	0.01	100	**Ga**	ppm	0.1	1000	**Ta**	ppm	0.06	2500
CaO	wt%	0.01	100	**Gd**	ppm	0.01	1000	**Tb**	ppm	0.005	1000
Na_2O	wt%	0.01	100	**Ge**	ppm	0.1	1000	**Th**	ppm	0.03	1000
K_2O	wt%	0.01	100	**Hf**	ppm	0.02	10000	**Ti**	ppm	6	50000
P_2O_5	wt%	0.01	100	**Ho**	ppm	0.003	1000	**Tl**	ppm	0.01	1000
SrO	wt%	0.01	100	**In**	ppm	0.04	1000	**Tm**	ppm	0.007	1000
BaO	wt%	0.01	100	**La**	ppm	0.1	10000	**U**	ppm	0.008	1000
LOI	wt%	0.01	100	**Lu**	ppm	0.004	1000	**V**	ppm	4	10000
Ag	ppm	0.05	800	**Mo**	ppm	1	10000	**W**	ppm	0.5	10000
Ba	ppm	2	10000	**Nb**	ppm	0.04	2500	**Y**	ppm	0.04	10000
Be	ppm	0.2	1000	**Nd**	ppm	0.07	10000	**Yb**	ppm	0.01	1000
Ce	ppm	0.1	10000	**Ni**	ppm	5	10000	**Zn**	ppm	4	10000
Co	ppm	0.2	10000	**Pb**	ppm	2	10000	**Zr**	ppm	0.1	10000

Note that concentrations of major and minor elements expressed as oxides (in wt%) and LOI were determined at ALS Canada Ltd. in Vancouver, whereas concentrations of trace elements (in ppm) were determined by fusion-digestion of a separate aliquot (pulp split) at ALS Canada Ltd. in Perth, Australia.
Fe_2O_3(T), total Fe expressed as Fe^{3+} oxide.

until incipient dryness, and finally taking up the residue in 50% HCl. Four-acid digestion breaks down most minerals and hence provides a near-total recovery for most analytes. However, the 4A digestion does not fully dissolve massive sulphides and refractory Al, Ba, Cr, Nb, rare earth elements (REE), Sn, Ta, Ti, W, and Zr phases. Other limitations of 4A digestion include a loss of volatile As, Ge, Hg, Si, Se, Sb, Tl, and other elements due to the temperature of digestion (fuming) and incomplete dissolution or re-precipitation of some elements (e.g., Al, Ca, K, W) that form insoluble fluorides and other compounds (e.g., Halley, 2020). In contrast, fusion via melting of a 0.1 g sample mixed with a $LiBO_2$ + $Li_2B_4O_7$ flux in a furnace at 1025 °C, followed by digestion of the fused glass in a mixture of HNO_3 + HF + HCl acids typically fully breaks down refractory minerals such as zircon, barite, and rare-metal oxides and thus provides total determinations (TD) for most analytes, although base metals are not fully recovered by the fusion technique. However, a trade-off with lithium borate fusion is typically higher minimum detection limits and generally poorer precision due to the increasing matrix interferences during the analysis compared with the 4A method (e.g., Halley, 2020).

Following the 4A or fusion digestion, the supernatant solutions were analyzed by a combination of inductively coupled plasma atomic emission spectroscopy (ICP-AES) and inductively coupled plasma mass spectrometry (ICP-MS) for up to 60 analytes (Tables 1 and 2). Using an ICP-MS coupled with a collision/reaction gas cell and an improved sample introduction method minimizes the oxide and polyatomic interferences, thereby achieving lower detection limits and a wide dynamic range. A typical 4A digestion combined with ICP-AES and ICP-MS provides minimum detection limits for trace elements one order of magnitude higher than those by 'super-trace' 4A with a combination of ICP-AES and ICP-MS finish (Table 1). Similar to the 4A method, the use of an ultra-pure flux and a clean laboratory for the 'super-trace' Li-borate fusion with ICP-MS finish also provides lower detection limits (Table 2) compared to typical Li-borate fusion ICP-MS. Although not total, the 'super-trace' 4A digestion combined with ICP-MS can better resolve trace-element patterns near detection limits than a standard Li-borate fusion combined with ICP-MS, but the fusion will provide more accurate determinations of major and refractory trace elements (e.g., Halley, 2020).

ALS Canada Ltd. performed the analysis at two different laboratories. Sample splits for concentrations of major and minor oxides by fusion with ICP-AES and for concentrations of 60 analytes by 4A digestion with ICP-AES and ICP-MS finish were analyzed at the ALS Geochemistry laboratory in Vancouver, B.C. Gravimetric loss on ignition (LOI) at 1000 °C for one hour was determined in the same laboratory. Sample splits for concentrations of trace elements by Li-borate fusion with ICP-MS finish were analyzed at the ALS Geochemistry laboratory in Perth, Australia.

4. Quality control methods and results

4.1. Quality control

A total of 87 blind quality controls were inserted, including pulp duplicates, preparation blanks, and certified reference materials as standards. Table 3 provides a statistical summary of the preparation blanks. Table 4 summarizes the estimated analytical precision and accuracy based on duplicates and standards as discussed below.

4.1.1. Preparation blanks

We analyzed Sigma-Aldrich certified (trace metals basis), silica sand (≥99.995 wt% SiO_2) to monitor contamination due to pulverizing samples using tungsten carbide or chromium steel ring and puck mill. A total of 38 splits (13 to 15 g) of the material were randomly inserted in the analytical batch at the rate of one blank sample per 25 routine samples. Despite our effort to minimize contamination, results from the blanks show mill-specific contamination. The tungsten carbide mill introduced Co (up to 102 ppm), Re (up to 0.008 ppm), Ta (up to 0.74 ppm), and W (up to 1015 ppm) contamination, and the chromium steel mill introduced Cr (up to 294 ppm), Fe (up to 0.2 wt.%), Mn (up to 9.7 ppm), Mo (up to 0.4 ppm), Ni (up to 8 ppm), V (up to 6 ppm), and Y (up to 0.43 ppm) contamination (Table 3). Except for Co, Cr, Re, and W, this contamination is below the average concentration for continental crust (Rudnick and Gao, 2005). Furthermore, typically a much larger mass of a routine sample relative to that of the blanks renders the impact of contamination variable to negligible, depending on sample composition. Nevertheless, Cr results should be used with caution for samples pulverized in a Cr-steel mill (Rukhlov et al., 2020). Likewise, Co, Re, and especially W results may be suspect for samples pulverized in a W-carbide mill. Despite a few ore-grade samples in the analytical batch, the blanks rule out any notable carry over contamination, demonstrating that the preparation procedure is adequate.

4.1.2. Precision

To monitor the analytical precision, 38 duplicate splits of pulverized material were randomly inserted, with one duplicate per block of 25 routine samples. Relative analytical precision is estimated in terms of the average coefficient of variation, CV_{AVR} (%), based on a total of 47 data pairs for duplicate samples (routine-duplicate pairs and repeat analyses of standards)

$$CV_{AVR}\ (\%) = 100\sqrt{\frac{2}{N}\sum_{i=1}^{N}\left(\frac{(a_i-b_i)^2}{(a_i+b_i)^2}\right)} \qquad \text{Eqn. 1}$$

where a_i and b_i are the analytical results for the ith pair of duplicate samples, and N is the number of the data pairs (Abzalov, 2008). We consider that CV_{AVR} values of less than 20% indicate generally acceptable precision. For the 4A method, the CV_{AVR} values are below the 20% threshold for all analytes, except for Re, Se, and Te (Table 4). Similarly, most analytes determined by TD methods show good precision, yielding the CV_{AVR} values below <20%, except for Cr_2O_3, In, Mo, and Sc. The relatively poor precision for these elements by TD compared with that by 4A might reflect interferences inherent to Li-fusion as discussed above.

4.1.3. Accuracy

To monitor the analytical accuracy (bias), splits of different certified reference materials were randomly inserted, with one standard for every set of 50-100 routine samples. The standards included the Canadian Certified Reference Materials Project

Table 3. Statistical summary of results for preparation blanks (silica).

Analyte	Method	Unit	W carbide mill (n = 14)			Cr steel mill (n = 24)		
			Median	Minimum	Maximum	Median	Minimum	Maximum
Ag	ME-MS61L	ppm	<0.002	<0.002	0.004	<0.002	<0.002	0.012
Al	ME-MS61L	wt%	0.01	<0.01	0.08	<0.01	<0.01	0.01
As	ME-MS61L	ppm	0.03	<0.02	0.07	0.09	0.06	0.2
Ba	ME-MS61L	ppm	<1	<1	4	<1	<1	2
Be	ME-MS61L	ppm	<0.02	<0.02	0.02	<0.02	<0.02	<0.02
Bi	ME-MS61L	ppm	<0.002	<0.002	0.006	<0.002	<0.002	0.008
Ca	ME-MS61L	wt%	<0.01	<0.01	0.07	<0.01	<0.01	0.01
Cd	ME-MS61L	ppm	<0.005	<0.005	<0.005	<0.005	<0.005	<0.005
Ce	ME-MS61L	ppm	0.06	0.04	0.57	0.05	0.01	0.38
Co	ME-MS61L	ppm	**96.8**	**71.9**	**99.1**	0.367	0.298	0.585
Cr	ME-MS61L	ppm	0.9	0.6	1.4	**233**	**180**	**274**
Cs	ME-MS61L	ppm	<0.01	<0.01	0.01	<0.01	<0.01	0.01
Cu	ME-MS61L	ppm	0.55	0.33	6.3	0.89	0.70	3.25
Fe	ME-MS61L	wt%	0.002	0.002	0.022	**0.173**	**0.138**	**0.199**
Ga	ME-MS61L	ppm	<0.05	<0.05	0.07	0.06	<0.05	0.10
Ge	ME-MS61L	ppm	<0.05	<0.05	0.05	<0.05	<0.05	<0.05
Hf	ME-MS61L	ppm	0.007	<0.004	0.01	0.006	0.004	0.009
In	ME-MS61L	ppm	<0.005	<0.005	<0.005	<0.005	<0.005	0.024
K	ME-MS61L	wt%	<0.01	<0.01	0.02	<0.01	<0.01	0.01
La	ME-MS61L	ppm	0.031	0.024	0.294	0.024	0.008	0.117
Li	ME-MS61L	ppm	<0.2	<0.2	0.2	<0.2	<0.2	0.3
Mg	ME-MS61L	wt%	<0.01	<0.01	0.04	<0.01	<0.01	<0.01
Mn	ME-MS61L	ppm	0.5	0.3	2.9	**7.7**	**6.3**	**9.7**
Mo	ME-MS61L	ppm	0.09	0.06	0.16	**0.33**	**0.18**	**0.40**
Na	ME-MS61L	wt%	0.003	<0.001	0.021	0.002	<0.001	0.006
Nb	ME-MS61L	ppm	<0.005	<0.005	0.015	0.014	0.008	0.057
Ni	ME-MS61L	ppm	0.78	0.65	8.55	**4.15**	**2.71**	**5.06**
P	ME-MS61L	wt%	<0.001	<0.001	0.001	<0.001	<0.001	<0.001
Pb	ME-MS61L	ppm	0.03	0.01	0.27	0.05	<0.01	0.19
Rb	ME-MS61L	ppm	0.02	<0.02	0.29	0.02	<0.02	0.2
Re	ME-MS61L	ppm	**0.0037**	**0.0027**	**0.0078**	<0.0004	<0.0004	0.0009
S	ME-MS61L	wt%	<0.01	<0.01	0.01	<0.01	<0.01	0.01
Sb	ME-MS61L	ppm	<0.02	<0.02	0.03	0.02	<0.02	0.03
Sc	ME-MS61L	ppm	0.01	<0.01	0.07	0.01	<0.01	0.04
Se	ME-MS61L	ppm	<0.006	<0.006	0.037	<0.006	<0.006	0.013
Sn	ME-MS61L	ppm	0.03	<0.02	0.06	0.07	0.05	0.1
Sr	ME-MS61L	ppm	0.18	0.09	1.02	0.19	0.08	1.69
Ta	ME-MS61L	ppm	0.01	<0.01	0.03	<0.01	<0.01	0.01
Te	ME-MS61L	ppm	<0.005	<0.005	<0.005	<0.005	<0.005	0.015
Th	ME-MS61L	ppm	0.014	0.009	0.034	0.018	0.01	0.027
Ti	ME-MS61L	ppm	<10	<10	10	<10	<10	10
Tl	ME-MS61L	ppm	<0.002	<0.002	0.003	<0.002	<0.002	0.003
U	ME-MS61L	ppm	<0.01	<0.01	0.01	<0.01	<0.01	0.04
V	ME-MS61L	ppm	0.1	0.1	0.7	**0.7**	**0.5**	**1.0**
W	ME-MS61L	ppm	**350**	**98.6**	**830**	0.038	0.029	0.201
Y	ME-MS61L	ppm	0.02	0.01	0.04	**0.12**	**0.01**	**0.29**
Zn	ME-MS61L	ppm	0.4	0.2	0.7	0.3	<0.2	1.8
Zr	ME-MS61L	ppm	0.2	0.1	0.8	0.2	0.1	0.4
Dy	MS61L-REE	ppm	<0.005	<0.005	0.013	<0.005	<0.005	0.013
Er	MS61L-REE	ppm	<0.004	<0.004	0.004	<0.004	<0.004	0.005
Eu	MS61L-REE	ppm	<0.004	<0.004	0.01	<0.004	<0.004	0.005
Gd	MS61L-REE	ppm	<0.005	<0.005	0.043	0.006	<0.005	0.01
Ho	MS61L-REE	ppm	<0.002	<0.002	0.002	<0.002	<0.002	0.002
Lu	MS61L-REE	ppm	<0.002	<0.002	<0.002	<0.002	<0.002	<0.002
Nd	MS61L-REE	ppm	0.026	0.013	0.303	0.023	<0.005	0.067
Pr	MS61L-REE	ppm	0.005	<0.004	0.073	0.006	<0.004	0.017
Sm	MS61L-REE	ppm	0.005	<0.004	0.065	0.006	<0.004	0.016
Tb	MS61L-REE	ppm	<0.002	<0.002	0.004	<0.002	<0.002	0.002
Tm	MS61L-REE	ppm	<0.002	<0.002	<0.002	<0.002	<0.002	0.002
Yb	MS61L-REE	ppm	<0.004	<0.004	<0.004	<0.004	<0.004	0.009
SiO_2	ME-ICP06	wt%	99.5	98.1	100	99.1	96.6	100
TiO_2	ME-ICP06	wt%	<0.01	<0.01	<0.01	<0.01	<0.01	0.01
Al_2O_3	ME-ICP06	wt%	0.02	<0.01	0.03	0.01	<0.01	0.06
Cr_2O_3	ME-ICP06	wt%	<0.002	<0.002	0.003	**0.039**	**0.031**	**0.043**

Table 3. continued.

Analyte	Method	Unit	W carbide mill (n = 14)			Cr steel mill (n = 24)		
			Median	Minimum	Maximum	Median	Minimum	Maximum
Fe_2O_3(T)	ME-ICP06	wt%	0.01	<0.01	0.06	**0.26**	**0.21**	**0.28**
MnO	ME-ICP06	wt%	<0.01	<0.01	0.01	<0.01	<0.01	0.01
MgO	ME-ICP06	wt%	<0.01	<0.01	0.02	0.01	<0.01	0.04
CaO	ME-ICP06	wt%	0.01	<0.01	0.05	0.02	0.01	0.03
Na_2O	ME-ICP06	wt%	<0.01	<0.01	0.22	0.01	<0.01	0.03
K_2O	ME-ICP06	wt%	0.03	0.01	0.06	0.02	<0.01	0.04
P_2O_5	ME-ICP06	wt%	<0.01	<0.01	0.02	<0.01	<0.01	0.02
SrO	ME-ICP06	wt%	<0.01	<0.01	<0.01	<0.01	<0.01	<0.01
BaO	ME-ICP06	wt%	<0.01	<0.01	<0.01	<0.01	<0.01	<0.01
LOI	OA-GRA05	wt%	0.09	<0.01	0.4	<0.02	<0.09	0.09
Ag	ME-MS81s	ppm	<0.05	<0.05	0.06	<0.05	<0.05	0.15
Ba	ME-MS81s	ppm	<2	<2	3	<2	<2	2
Be	ME-MS81s	ppm	<0.2	<0.2	<0.2	<0.2	<0.2	<0.2
Ce	ME-MS81s	ppm	0.1	<0.1	0.2	0.1	<0.1	0.5
Co	ME-MS81s	ppm	**87.5**	**64.8**	**101.5**	0.4	0.3	0.5
Cr	ME-MS81s	ppm	<3	<3	4	**255**	**215**	**294**
Cs	ME-MS81s	ppm	<0.04	<0.04	<0.04	<0.04	<0.04	<0.04
Cu	ME-MS81s	ppm	<3	<3	7	<3	<3	7
Dy	ME-MS81s	ppm	<0.02	<0.02	<0.02	<0.02	<0.02	0.02
Er	ME-MS81s	ppm	<0.02	<0.02	<0.02	<0.02	<0.02	<0.02
Eu	ME-MS81s	ppm	<0.01	<0.01	0.01	<0.01	<0.01	<0.01
Ga	ME-MS81s	ppm	<0.1	<0.1	<0.1	0.1	<0.1	0.1
Gd	ME-MS81s	ppm	<0.01	<0.01	0.02	0.01	<0.01	0.03
Ge	ME-MS81s	ppm	0.7	0.6	0.8	0.8	0.6	0.9
Hf	ME-MS81s	ppm	0.04	0.02	0.06	0.05	0.03	0.07
Ho	ME-MS81s	ppm	<0.003	<0.003	0.003	<0.003	<0.003	0.006
In	ME-MS81s	ppm	<0.04	<0.04	<0.04	<0.04	<0.04	<0.04
La	ME-MS81s	ppm	0.1	<0.1	0.3	0.1	<0.1	0.5
Lu	ME-MS81s	ppm	<0.004	<0.004	<0.004	<0.004	<0.004	0.006
Mo	ME-MS81s	ppm	<1	<1	2	1	<1	1
Nb	ME-MS81s	ppm	0.04	<0.04	0.08	<0.04	<0.04	0.06
Nd	ME-MS81s	ppm	<0.07	<0.07	0.11	<0.07	<0.07	0.13
Ni	ME-MS81s	ppm	<5	<5	9	5	<5	8
Pb	ME-MS81s	ppm	<2	<2	5	<2	<2	<2
Pr	ME-MS81s	ppm	<0.02	<0.02	0.03	<0.02	<0.02	0.04
Rb	ME-MS81s	ppm	0.1	<0.1	0.2	<0.1	<0.1	0.1
Sc	ME-MS81s	ppm	1.1	0.6	1.3	1.3	0.7	1.5
Sm	ME-MS81s	ppm	<0.01	<0.01	0.03	0.01	<0.01	0.04
Sn	ME-MS81s	ppm	<0.5	<0.5	<0.5	<0.5	<0.5	<0.5
Sr	ME-MS81s	ppm	0.2	<0.2	0.7	0.2	<0.2	0.8
Ta	ME-MS81s	ppm	**0.60**	**0.51**	**0.74**	<0.06	<0.06	<0.06
Tb	ME-MS81s	ppm	<0.005	<0.005	<0.005	<0.005	<0.005	0.005
Th	ME-MS81s	ppm	0.03	<0.03	0.05	<0.03	<0.03	0.13
Ti	ME-MS81s	ppm	<6	<6	6	<6	<6	16
Tl	ME-MS81s	ppm	0.01	<0.01	0.03	<0.01	<0.01	0.01
Tm	ME-MS81s	ppm	<0.007	<0.007	<0.007	<0.007	<0.007	<0.007
U	ME-MS81s	ppm	0.008	<0.008	0.01	0.008	<0.008	0.019
V	ME-MS81s	ppm	<4	<4	5	<4	<4	6
W	ME-MS81s	ppm	**935**	**730**	**1015**	<0.5	<0.5	1.1
Y	ME-MS81s	ppm	<0.04	<0.04	0.08	0.15	<0.04	0.43
Yb	ME-MS81s	ppm	<0.01	<0.01	0.01	<0.01	<0.01	0.01
Zn	ME-MS81s	ppm	<4	<4	<4	<4	<4	11
Zr	ME-MS81s	ppm	1.4	0.5	2.0	1.4	0.9	1.9

Analytical method codes (ALS Canada Ltd.): **ME-MS61L**, HNO_3-$HClO_4$-HF acid digestion, followed by HCl leach and inductively coupled plasma mass spectrometry (ICP-MS) finish. **MS61L-REE**, rare earth element add-on package for ME-MS61L method. **ME-ICP06**, lithium borate fusion with ICP-AES finish. **OA-GRA05**, gravimetric loss on ignition at 1000 °C for one hour. **ME-MS81s**, lithium borate fusion with ICP-MS finish. Red values indicate contamination by the mill.

'<' denotes values below the minimum detection limit.

Table 4. Estimated analytical precision and accuracy.

Analyte	Method	CV_{AVR} (%) n = 47	TDB-1 n = 3	SY-4 n = 3	RGM-2 n = 3	GSP-2 n = 1	WPR-1a n = 1
Ag	ME-MS61L	9.1	na	1.84	na	na	0.00
Al	ME-MS61L	1.9	0.22	14.80	0.80	0.19	0.05
As	ME-MS61L	16.8	0.41	0.49	0.08	na	0.12
Ba	ME-MS61L	2.1	0.42	0.15	0.25	0.38	0.47
Be	ME-MS61L	2.2	na	0.08	0.95	0.40	na
Bi	ME-MS61L	9.4	na	0.98	na	na	0.47
Ca	ME-MS61L	1.9	0.26	1.57	0.29	0.61	0.13
Cd	ME-MS61L	17.3	na	0.53	na	na	0.02
Ce	ME-MS61L	5.4	0.24	5.15	0.33	0.20	1.04
Co	ME-MS61L	2.9	0.46	1.62	0.01	0.10	0.03
Cr	ME-MS61L	6.7	2.58	2.31	na	0.30	1.77
Cs	ME-MS61L	4.0	na	0.39	na	0.93	0.34
Cu	ME-MS61L	3.6	0.40	2.04	0.15	0.15	0.15
Fe	ME-MS61L	1.6	1.11	5.09	0.33	0.16	0.18
Ga	ME-MS61L	3.3	0.34	0.72	0.02	0.00	0.91
Ge	ME-MS61L	16.1	na	0.78	na	na	na
Hf	ME-MS61L	4.9	0.72	11.36	0.24	6.64	1.85
In	ME-MS61L	10.4	na	0.46	na	na	0.47
K	ME-MS61L	3.1	0.34	1.30	0.10	0.16	0.17
La	ME-MS61L	6.2	0.38	6.46	0.44	0.76	1.26
Li	ME-MS61L	1.8	0.14	0.43	0.44	0.08	0.25
Mg	ME-MS61L	7.2	0.50	4.60	0.50	0.11	0.06
Mn	ME-MS61L	5.9	1.12	2.15	0.57	0.05	0.33
Mo	ME-MS61L	9.1	0.34	0.51	0.02	0.01	na
Na	ME-MS61L	2.5	0.32	0.65	0.16	0.00	0.12
Nb	ME-MS61L	4.4	na	0.03	na	1.22	0.38
Ni	ME-MS61L	13.6	0.16	1.46	na	0.29	0.03
P	ME-MS61L	1.9	0.38	1.33	0.00	0.10	0.33
Pb	ME-MS61L	5.9	0.21	0.43	0.34	0.46	0.47
Rb	ME-MS61L	4.7	0.74	5.69	0.73	0.96	0.75
Re	ME-MS61L	21.6	na	na	na	na	na
S	ME-MS61L	14.4	na	0.15	na	na	0.44
Sb	ME-MS61L	14.1	0.33	0.50	na	na	0.11
Sc	ME-MS61L	4.5	0.12	1.77	0.66	0.36	0.17
Se	ME-MS61L	37.8	na	0.48	na	na	0.04
Sn	ME-MS61L	3.7	0.04	0.25	1.07	na	0.52
Sr	ME-MS61L	2.8	0.01	0.35	0.35	0.33	0.39
Ta	ME-MS61L	4.9	0.22	0.78	na	na	1.28
Te	ME-MS61L	22.9	na	na	na	na	0.04
Th	ME-MS61L	7.6	0.50	1.35	0.39	0.65	0.95
Ti	ME-MS61L	4.6	0.26	1.20	0.72	0.57	0.48
Tl	ME-MS61L	4.6	na	0.32	na	na	1.11
U	ME-MS61L	11.2	0.66	1.06	0.30	1.39	na
V	ME-MS61L	3.5	0.94	0.80	na	0.22	0.09
W	ME-MS61L	12.3	na	0.51	na	na	na
Y	ME-MS61L	3.5	0.38	7.66	0.33	1.49	0.72
Zn	ME-MS61L	4.6	0.05	0.13	0.33	0.36	0.10
Zr	ME-MS61L	4.5	0.22	13.63	0.36	8.62	3.32
Dy	MS61L-REE	4.7	0.82	2.25	0.73	na	0.37
Er	MS61L-REE	4.3	na	1.84	0.76	na	0.96
Eu	MS61L-REE	3.6	0.78	3.28	0.58	1.09	0.91
Gd	MS61L-REE	5.1	na	2.53	0.10	0.22	0.36
Ho	MS61L-REE	3.7	0.07	2.98	0.25	0.87	1.02
Lu	MS61L-REE	4.9	0.41	0.77	0.11	1.48	1.23
Nd	MS61L-REE	4.0	0.10	4.96	0.16	0.39	0.35
Pr	MS61L-REE	4.6	na	4.26	0.48	0.05	1.70
Sm	MS61L-REE	4.2	0.06	2.23	0.30	0.95	0.43
Tb	MS61L-REE	4.1	0.82	1.74	0.19	na	0.90
Tm	MS61L-REE	4.1	0.59	1.74	na	1.96	0.57
Yb	MS61L-REE	4.4	0.29	1.00	na	1.13	1.08
SiO_2	ME-ICP06	0.8	0.41	2.03	0.08	0.10	0.00
TiO_2	ME-ICP06	1.7	0.18	1.07	0.36	0.88	0.00
Al_2O_3	ME-ICP06	1.0	0.05	0.26	0.62	1.02	0.13
Cr_2O_3	ME-ICP06	22.7	0.25	0.88	na	0.00	0.09

Table 4. continued.

Analyte	Method	CV_{AVR} (%) n = 47	TDB-1 n = 3	SY-4 n = 3	RGM-2 n = 3	GSP-2 n = 1	WPR-1a n = 1
Fe_2O_3(T)	ME-ICP06	1.1	0.94	0.41	0.33	0.06	0.68
MnO	ME-ICP06	10.4	0.50	0.60	0.24	0.10	0.18
MgO	ME-ICP06	1.7	0.05	1.25	0.08	0.15	0.20
CaO	ME-ICP06	3.3	0.13	0.87	0.32	0.00	0.09
Na_2O	ME-ICP06	8.8	0.17	0.90	0.18	0.22	0.24
K_2O	ME-ICP06	3.8	0.33	0.07	0.04	0.14	1.15
P_2O_5	ME-ICP06	5.3	0.40	0.70	0.12	0.41	0.09
SrO	ME-ICP06	9.5	0.04	0.30	1.50	1.86	2.77
BaO	ME-ICP06	1.8	1.50	1.00	0.75	0.00	2.99
LOI	OA-GRA05	12.6	0.49	0.03	na	na	0.12
Ag	ME-MS81s	18.9	na	1.72	na	na	2.06
Ba	ME-MS81s	6.2	0.62	0.02	0.08	0.48	0.83
Be	ME-MS81s	7.8	na	2.50	0.94	0.21	na
Ce	ME-MS81s	6.5	0.41	0.27	0.55	0.76	0.75
Co	ME-MS81s	5.3	0.30	1.31	0.00	0.06	0.30
Cr	ME-MS81s	10.8	0.06	0.84	na	0.08	0.14
Cs	ME-MS81s	10.0	na	0.09	na	0.27	0.46
Cu	ME-MS81s	7.8	0.24	0.78	0.61	0.37	1.13
Dy	ME-MS81s	9.8	0.79	0.42	0.92	na	0.24
Er	ME-MS81s	11.7	na	0.67	1.20	na	0.32
Eu	ME-MS81s	11.6	1.16	0.18	0.95	0.15	0.62
Ga	ME-MS81s	7.9	0.02	0.53	0.29	0.38	0.37
Gd	ME-MS81s	7.9	na	0.41	0.18	0.02	0.30
Ge	ME-MS81s	8.3	na	0.41	na	na	na
Hf	ME-MS81s	6.4	0.51	0.07	0.04	0.65	0.22
Ho	ME-MS81s	10.0	0.01	0.75	0.11	0.04	0.27
In	ME-MS81s	22.4	na	0.50	na	na	0.40
La	ME-MS81s	7.5	0.25	0.20	0.43	0.36	0.61
Lu	ME-MS81s	11.8	0.66	0.30	0.46	0.26	0.57
Mo	ME-MS81s	25.4	0.43	0.40	0.50	0.06	na
Nb	ME-MS81s	12.1	na	0.11	na	0.09	0.65
Nd	ME-MS81s	7.2	0.07	0.02	0.42	0.28	0.55
Ni	ME-MS81s	6.0	0.19	0.62	na	0.22	0.70
Pb	ME-MS81s	15.1	0.37	0.62	1.25	0.31	1.25
Pr	ME-MS81s	6.5	na	0.28	0.41	0.58	0.47
Rb	ME-MS81s	6.6	0.66	0.67	0.09	0.03	0.81
Sc	ME-MS81s	32.8	0.21	0.05	0.53	0.05	0.12
Sm	ME-MS81s	11.0	0.39	0.26	0.24	0.03	0.30
Sn	ME-MS81s	18.8	0.10	0.44	1.20	na	0.52
Sr	ME-MS81s	6.4	0.22	0.32	0.18	0.08	0.37
Ta	ME-MS81s	9.0	0.21	0.61	na	na	1.05
Tb	ME-MS81s	8.0	0.74	0.55	0.00	na	0.28
Th	ME-MS81s	5.8	0.20	0.08	0.27	0.41	0.03
Ti	ME-MS81s	7.2	0.79	4.10	1.10	0.69	0.36
Tl	ME-MS81s	17.4	na	0.80	na	na	0.19
Tm	ME-MS81s	7.8	0.50	0.14	na	0.10	0.21
U	ME-MS81s	6.3	0.56	0.31	0.16	0.26	na
V	ME-MS81s	14.9	0.06	0.11	na	0.11	0.07
W	ME-MS81s	15.6	na	0.48	na	na	na
Y	ME-MS81s	8.3	0.44	0.84	0.67	0.22	0.71
Yb	ME-MS81s	7.2	0.11	0.46	na	0.23	0.31
Zn	ME-MS81s	7.5	0.03	0.65	0.43	0.04	0.45
Zr	ME-MS81s	7.4	0.17	0.49	0.01	0.75	0.60

Analytical method codes (ALS Canada Ltd.): **ME-MS61L**, HNO_3-$HClO_4$-HF acid digestion, followed by HCl leach with inductively coupled plasma atomic emission spectroscopy (ICP-AES) and inductively coupled plasma mass spectrometry (ICP-MS) finish. **MS61L-REE**, rare earth element add-on package for ME-MS61L method. **ME-ICP06**, lithium borate fusion with ICP-AES finish. **OA-GRA05**, gravimetric loss on ignition at 1000 °C for one hour. **ME-MS81s**, lithium borate fusion with ICP-MS finish.
n, number of duplicate pairs or replicate analyses of standards.
'na' denotes not analyzed or uncertified analytes.

(CCRMP) diabase TDB-1 (3 splits; Sen Gupta, 1994), diorite gneiss SY-4 (3 splits; Bowman, 1995), and peridotite WPR-1a (1 split; Leaver and Salley, 2012), and the United States Geological Survey (USGS) rhyolite RGM-2 (3 splits; Wilson, 2009), and granodiorite GSP-2 (1 split; Wilson, 1998). For replicate analyses of standards, accurate or unbiased analytical results satisfy the following condition.

$$\frac{|m-\mu|}{2\sqrt{{\sigma_L}^2+\frac{{S_w}^2}{n}}} \leq 1 \qquad \text{Eqn. 2}$$

where μ is the certified mean of a standard, σ_L is the certified inter-laboratory standard deviation or 95% confidence interval of a standard, m is the average of the replicate analyses of the standard included in the analytical batch, S_w is the standard deviation or 95% confidence interval of the replicate analyses of the standard in the batch, and n is the number of replicate analyses of the standard in the batch (Abzalov, 2008). 'Information' values without uncertainties for the standards were excluded from the accuracy test. Lithium-borate fusion and LOI provided more accurate total determinations than the 4A digestion, especially for major elements and trace elements that are hosted mainly by refractory phases (e.g., Al, Cr, Fe, Hf, Mg, Mn, Rb, REE, Zr; Table 4).

4.2. Results

The 4A technique has been increasingly popular in mineral exploration because it is less expensive than TD methods, provides determinations for many analytes, and yields low minimum detection limits (e.g., Halley, 2020). However, scatterplots for selected elements determined by TD versus 4A reveal under-recovery of Zr, Ti, Ba, and Al by 4A digestion (Fig. 3). These elements are hosted by refractory minerals such as zircon, titanite, and barite that do not fully dissolve in acids.

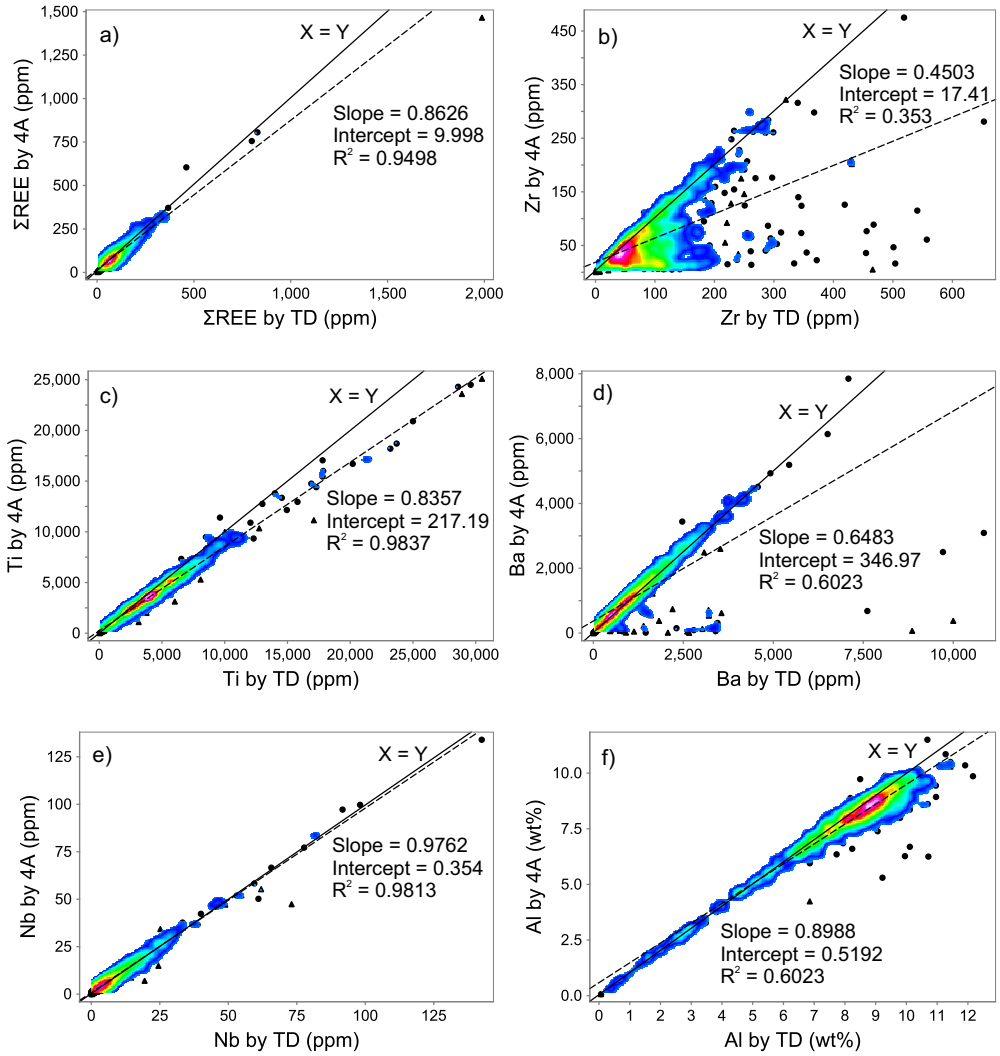

Fig. 3. Scatterplots for concentrations of selected elements by total determination (TD) vs four-acid digestion (4A) and inductively coupled plasma mass spectrometry (ICP-MS), or inductively coupled plasma atomic emission spectroscopy (ICP-AES) in rock samples from northwestern British Columbia (n = 984), gridded point density, X = Y (solid line), and least squares regression (dashed line) and statistics. Symbols by sample purpose: petrogenesis (dots), alteration and/or mineralization (triangles). **a)** Sum of lanthanides (∑REE) by TD (ppm) versus ∑REE by 4A (ppm). **b)** Zr by TD (ppm) versus Zr by 4A (ppm). **c)** Ti by TD (ppm) versus Ti by 4A (ppm). **d)** Ba by TD (ppm) versus Ba by 4A (ppm). **e)** Nb by TD (ppm) versus Nb by 4A (ppm). **f)** Al by TD (wt%) versus Al by 4A (wt%).

Others may precipitate as insoluble tungstate, perchlorates, and fluorides (e.g., Al) during the 4A digestion. Silica is not reported by 4A due to SiF_6 fuming. Although Halley (2000) suggested that Sc determined by 4A may be used as a proxy for SiO_2, samples analyzed by 4A in this study (n = 984), including duplicates, show an excessive scatter ($R^2 = 0.3992$) on a plot of SiO_2 versus Sc (Fig. 4).

Mineral prospectivity diagrams using data from both 4A and TD (Fig. 5) show that many samples overlap with compositions for fertile porphyry Cu magmas (Richards and Kerrich, 2007;

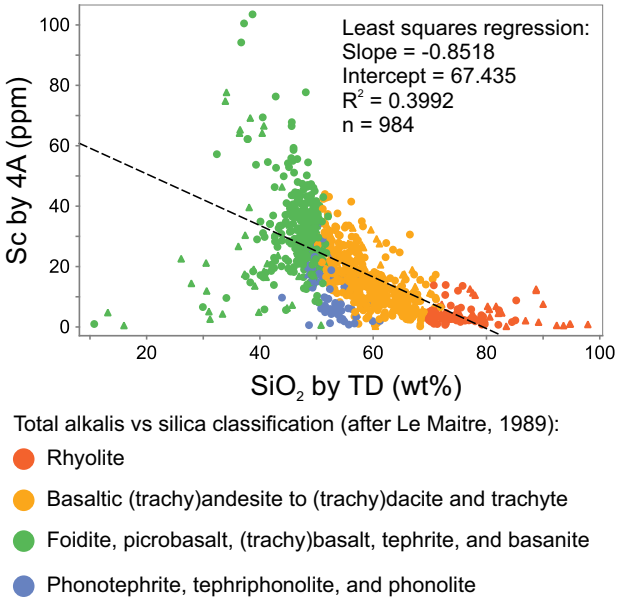

Fig. 4. SiO_2 (wt%) by total determination (TD) versus Sc (ppm) by four-acid digestion (4A), least squares regression (dashed line), and statistics. Total alkalis versus silica classification after Le Maitre (1989) in colour; dots are petrogenesis samples, triangles are altered and/or mineralized rocks.

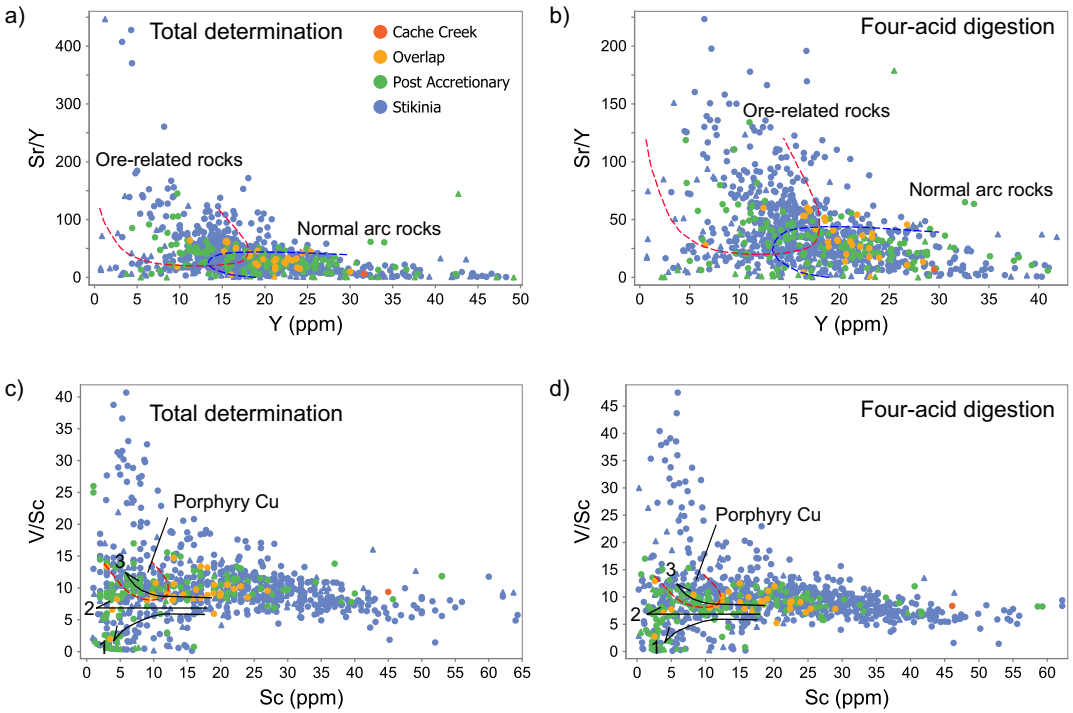

Fig. 5. Comparison of analytical methods in terms of petrogenetic discrimination diagrams for rock samples within Mahalanobis distance at chi-squared cut-off value $p = 0.99$ (De Maesschalck et al., 2000). **a)** Y (ppm) versus Sr/Y by total determination. **b)** Y (ppm) versus Sr/Y by four-acid digestion. Fields of normal arc rocks (blue outline) and ore-related rocks (red outline) after Richards and Kerrich (2007). **c)** Sc (ppm) versus V/Sc by total determination. **d)** Sc (ppm) versus V/Sc by four-acid digestion. Prospective porphyry copper deposit field (red outline) and fractional crystallization trends (black arrows) of magnetite (1), ilmenite (2), and hornblende and/or clinopyroxene (3) after Halley (2020). Classification of points by terranes in northwestern British Columbia in colour and by sample purpose in symbol shape: petrogenesis (dots) and alteration/mineralization (triangles).

Halley, 2020). In terms of Sr/Y ratio, TD results (Fig. 5a) show twice the range of values compared with that of 4A (Fig. 5b). TD data also show a higher proportion of data points with K/Al molar ratio > 0.5 (Fig. 6a) compared with that of 4A (Fig. 6b). In general, both TD and 4A results appear to show a similar degree of scatter in terms of Sc versus V/Sc (Figs. 5c and d) and Al-K-Mg (Figs. 6c and d), but differences emerge when comparing the data on a sample-by-sample basis. Petrogenetic samples show the same magnitude of scatter in terms of major and trace elements as altered and mineralized samples originally assayed for their metal contents.

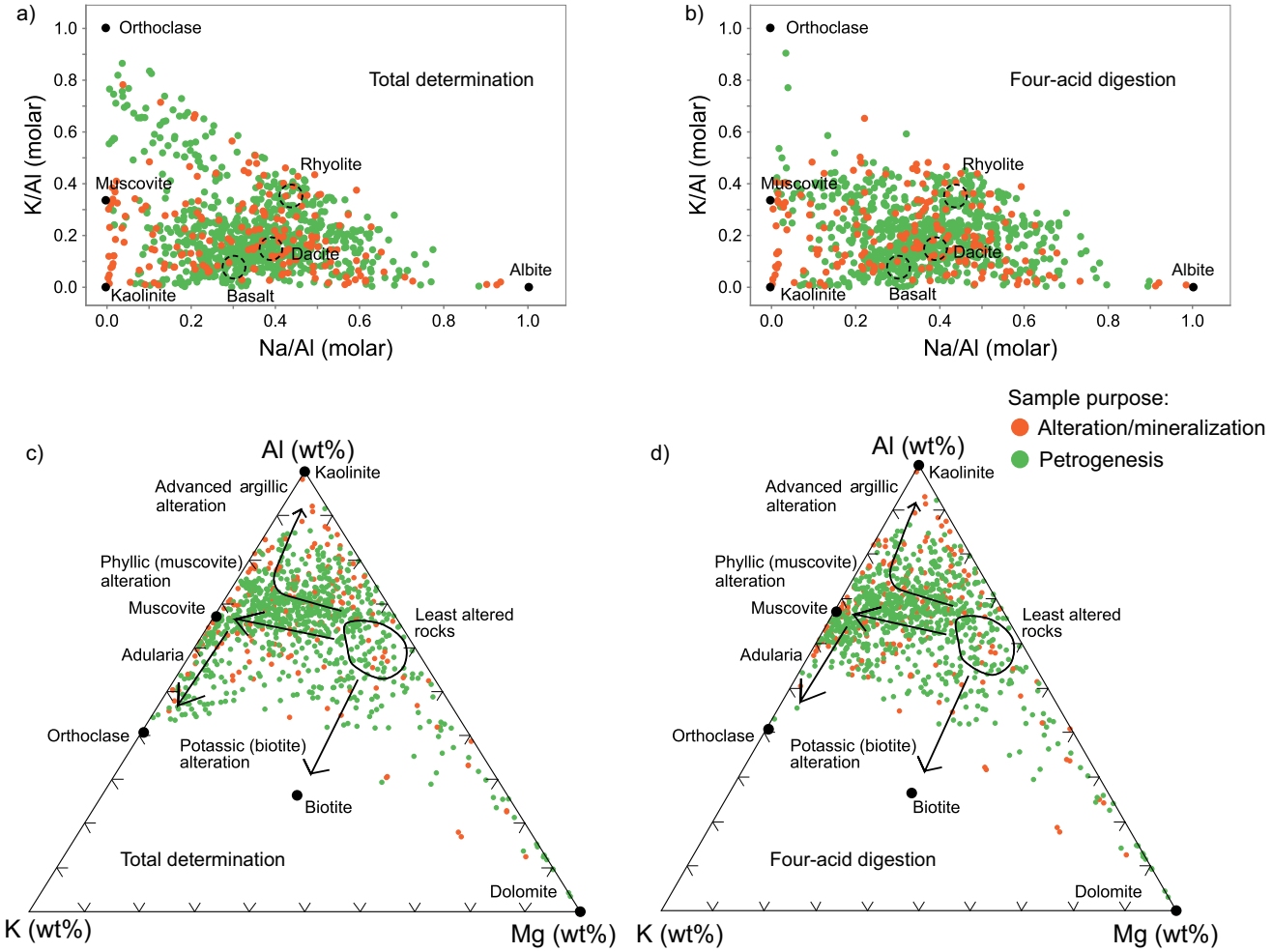

Fig. 6. Comparison of analytical methods in terms of alteration discrimination diagrams for rock samples. **a)** Na/Al (molar) versus K/Al (molar) by total determination. **b)** Na/Al (molar) versus K/Al (molar) by four-acid digestion. Fields of unaltered basalt, dacite, and rhyolite after Cox et al. (1979). **c)** Al-K-Mg ternary (wt%) by total determination. **d)** Al-K-Mg ternary (wt%) by four-acid digestion. Field of least altered rocks and adularia, advanced argillic, phyllic (muscovite), and potassic (biotite) alteration trends after Scott Halley (ioGAS software version 7.4.2).

5. Conclusion

This release follows up and extends van Straaten et al. (2022a) by providing a new lithogeochemical dataset for 946 BCGS archived samples (plus 87 quality controls) from northwestern British Columbia with comprehensive geoscientific metadata. Samples were reanalyzed using modern 4A and Li-borate fusion (498 samples) methods for up to 60 analytes, each with the lowest commercially available minimum detection limits.

Acknowledgements

Newcrest Mining Ltd. is thanked for providing financial support for re-analysis and geoscience assistant salary. We thank Iyad Al Khatib (ALS Geochemistry) for discussions of the analytical methods and for overseeing the analysis at the ALS Canada Ltd., Tian Han (BCGS) for retrieving records from the BC rock geochemical database, and Yao Cui for help with the BC digital geology database. We also thank Andrejs Panteleyev (XDM Geo Consulting) and Ray Lett (BCGS, Emeritus Scientist) for their comments regarding the archive samples, and Sarah Shea (Corporate Information and Records Management Office, Citizens' Services) for providing access to the BC Archives and their secure microfilms. We are grateful to Neil Wildgust (BCGS) and Lawrence Aspler (BCGS) for critical review and comments that improved the final report.

References cited

Abzalov, M., 2008. Quality control of assay data: A review of procedures for measuring and monitoring precision and accuracy. Exploration and Mining Geology, 17, 131–144. https://doi.org/10.2113/gsemg.17.3-4.131

Alldrick, D.J., Nelson, J.L., Barresi, T., Stewart, M.L., and Simpson, K.A., 2006. Geology of the Upper Iskut River area, British Columbia. British Columbia Ministry of Energy, Mines and Petroleum Resources, British Columbia Geological Survey Open File 2006-02, 1:100,000 scale.

Ash, C.H., MacDonald, R.W.J., Stinson, P.K., Fraser, T.M., Nelson, K.J., Arden, K.M., and Lefebure, D.V., 1997. Geology and mineral occurrences of the Tatogga Lake area (NTS 104H/12NW, 13SW & 104G/9NE, 16SE). British Columbia Ministry of Employment and Investment, British Columbia Geological Survey Open File 1997-03, 1:100,000 scale.

Bowman, W.S., 1995. Canadian diorite gneiss SY-4: Preparation and certification by eighty-nine international laboratories. Geostandards Newsletter, 19, 101-124.

Brown, D.A., Gunning, M.H., and Greig, C.J., 1996. The Stikine project: Geology of western Telegraph Creek map area, northwestern British Columbia. British Columbia Ministry of Energy, Mines and Petroleum Resources, British Columbia Geological Survey Bulletin 95, 130 p.

Cohen, K.M., Finney, S.C., Gibbard, P.L., and Fan, J.-X., 2013. The ICS International chronostratigraphic chart. Episodes, 36, 199–204. Version 2021/10. https://stratigraphy.org/ICSchart/ChronostratChart2021-10.pdf

Cox, K.G., Bell, J.D., and Pankhurst, R.J., 1979. The interpretation of igneous rocks. Allen & Unwin, London, United Kingdom, 450 p.

Cui, Y., Miller, D., Schiarizza, P., and Diakow, L.J., 2017. British Columbia digital geology. British Columbia Ministry of Energy, Mines and Petroleum Resources, British Columbia Geological Survey Open File 2017-8, 9 p. Data version 2019-12-19.

Enns, S.G., Thompson, J.F.H., Stanley, C.R., and Yarrow, E.W., 1995. The Galore Creek porphyry copper-gold deposits, northwestern British Columbia. In: Schroeter, T.G. (Ed.), Porphyry Deposits of the Northwestern Cordillera of North America. Canadian Institute of Mining and Metallurgy, Special Volume 46, pp. 630-644.

De Maesschalck, R., Jouan-Rimbaud, D., and Massart, D.L., 2000. The Mahalanobis distance. Chemometrics and Intelligent Laboratory Systems, 50, 1-18.

Halley, S., 2020. Mapping magmatic and hydrothermal processes from routine exploration geochemical analyses. Economic Geology, 115, 489-503.

Han, T., and Rukhlov, A.S., 2020. Update of rock geochemical database at the British Columbia Geological Survey. British Columbia Ministry of Energy, Mines and Petroleum Resources, British Columbia Geological Survey GeoFile 2020-02, 4 p.

Han, T., Rukhlov, A.S., Naziri, M., and Moy, A., 2016. New British Columbia lithogeochemical database: Development and preliminary data release. British Columbia Ministry of Energy and Mines, British Columbia Geological Survey GeoFile 2016-4, 6 p.

Hunter, R.C., and van Straaten, B.I., 2020. Preliminary stratigraphy and geochronology of the Hazelton Group, Kitsault River area, Stikine terrane, northwest British Columbia. In: Geological Fieldwork 2019, British Columbia Ministry of Energy, Mines and Petroleum Resources, British Columbia Geological Survey Paper 2020–02, pp. 101–118.

Hunter, R.C., Sebert, C.F.B., Friedman, R., and Wall, C., 2022. Revised stratigraphy and geochronology of the Hazelton Group, host rocks for volcanogenic mineralization in the Kitsault River area, northwest British Columbia. In: Geological Fieldwork 2021, British Columbia Ministry of Energy, Mines and Low Carbon Innovation, British Columbia Geological Survey Paper 2022–01, pp. 63–81.

Leaver, M.E., and Salley, J., 2012. WPR-1a certified reference material for a peridotite with rare earth and platinum group elements. Natural Resources Canada, Canadian Certified Reference Materials Project, Certificate of Analysis, version April 2012, Ottawa, Ontario, Canada, 7 p.

Le Maitre, R.W. (Ed.), 1989. A classification of igneous rocks and glossary of terms. Recommendations of the IUGS Commission on the systematics of igneous rocks. Blackwell Science Inc., Oxford, United Kingdom, 206 p.

Logan, J.M., 2004. Geology and geochemistry of the Foremore area. British Columbia Ministry of Energy and Mines, British Columbia Geological Survey Open File 2004–11, 1:50,000 scale.

Logan, J.M., 2005. Alkaline magmatism and porphyry Cu-Au deposits at Galore Creek, northwestern British Columbia. In: Geological Fieldwork 2004, British Columbia Ministry of Energy and Mines, British Columbia Geological Survey Paper 2005-1, pp. 237-248.

Logan, J.M., and Koyanagi, V.M., 1994. Geology and mineral deposits of the Galore Creek area. British Columbia Ministry of Energy, Mines and Petroleum Resources, British Columbia Geological Survey, Bulletin 92, 102 p.

Logan, J.M., Drobe, J.R., and McClelland, W.C., 2000. Geology of the Forrest Kerr-Mess Creek area, northwestern British Columbia. British Columbia Ministry of Energy and Mines, British Columbia Geological Survey Bulletin 104, 132 p.

Logan, J.M., Moynihan, D.P., and Diakow, L.J., 2012. Dease Lake geoscience project, Part I: Geology and mineralization of the Dease Lake (NTS 104J/08) and East-Half of the Little Tuya River (NTS 104J/07E) map sheets, northern British Columbia. In: Geological Fieldwork 2011, British Columbia Ministry of Energy, Mines and Natural Gas, British Columbia Geological Survey Paper 2012-1, pp. 23-44.

Miller, E.A., Kennedy, L.A., and van Straaten, B.I., 2020. Geology of the Kinskuch Lake area and Big Bulk porphyry prospect: Syndepositional faulting and local basin formation during the Rhaetian (latest Triassic) transition from the Stuhini to the Hazelton Group. In: Geological Fieldwork 2019, British Columbia Ministry of Energy, Mines and Petroleum Resources, British Columbia Geological Survey Paper 2020-01, pp. 77-100.

Nelson, J., Waldron, J., van Straaten, B., Zagorevski, A., and Rees, C., 2018. Revised stratigraphy of the Hazelton Group in the Iskut River region, northwestern British Columbia. In: Geological Fieldwork 2017, British Columbia Ministry of Energy, Mines and Petroleum Resources, British Columbia Geological Survey Paper 2018-1, pp. 15-38.

North American Commission on Stratigraphic Nomenclature, 2005. North American Stratigraphic Code. American Association of Petroleum Geologists Bulletin, 89, 1547-1591. https://doi.org/10.1306/07050504129

Richards, J.P., and Kerrich, R., 2007. Special paper: Adakite-like rocks: Their diverse origins and questionable role in metallogenesis. Economic Geology 102, 537-576.

Rudnick, R.L., and Gao, S., 2005. Composition of the continental crust. In: Heinrich, D.H., Rudnick, R.L., and Turekian, K.K., (Eds.), The Crust. Treatise on Geochemistry, Volume 3, Elsievier, Amsterdam, pp. 1-64.

Rukhlov, A.S., Fortin, G., Kaplenkov, G.N., Lett, R.E., Lai, V. W.-M., and Weis, D., 2020. Multi-media geochemical and Pb isotopic evaluation of modern drainages on Vancouver Island. In: Geological Fieldwork 2019, British Columbia Ministry of Energy, Mines and Petroleum Resources, British Columbia Geological Survey Paper 2020-01, pp. 133-167.

Siivola, J., and Schmid, R., 2007. A systematic nomenclature for metamorphic rocks: 12. List of mineral abbreviations. Recommendations by the IUGS Subcommission on the Systematics of Metamorphic Rocks: Web version 01.02.2007,14 p. http://www.ngdc.nerc.ac.uk/scmr/docs/papers/paper_12.pdf

van Straaten, B.I., Logan, J.M., and Diakow, L.J., 2012. Mesozoic magmatism and metallogeny of the Hotailuh Batholith, northwestern British Columbia. British Columbia Ministry of Energy, Mines and Natural Gas, British Columbia Geological Survey Open File 2012-06, 58 p.

van Straaten, B.I., Logan, J.M., Hunter, R.C., Nelson, J.L., and Miller, E.A., 2022a. Igneous lithogeochemistry data for the Dease Lake, Kitsault River, Galore Creek, Telegraph Creek, Foremore, and other areas in northwestern British Columbia. British Columbia Ministry of Energy, Mines and Low Carbon Innovation, British Columbia Geological Survey GeoFile 2022-12, 14 p.

van Straaten, B.I., Logan, J.M., Nelson, J.L., Moynihan, D.P., Diakow, L.J., Gibson, R., Bichlmaier, S.J., Wearmouth, C.D., Friedman, R.M., Golding, M.L., Miller, E.A., and Poulton, T.P., 2022b. Bedrock geology of the Dease Lake area. British Columbia Ministry of Energy, Mines and Low Carbon Innovation, British Columbia Geological Survey Geoscience Map 2022–01, 1:100,000 scale.

BRITISH COLUMBIA
Ministry of Energy, Mines and Low Carbon Innovation

BRITISH COLUMBIA est. 1895 GEOLOGICAL SURVEY